

Synthesis, Characterization and Antibacterial Effect of Nanoparticles Core Shell Ag@ZnO

Renzo Cabrera-Pinedo^a, Gina Zavaleta-Espejo^{a,c,*}, José Saldaña-Jiménez^{a,c}, Segundo R. Jáuregui-Rosas^{b,c}, Fanny Samanamud-Moreno^{b,c}, Hector Felix-Quintero^d, Gelsi Espino-Caballero^a

^aLaboratory of Biotechnology and Animal Reproduction, National University of Trujillo, La Libertad, Perú.

^bDepartament of Physics, National University of Trujillo, La Libertad, Perú

^cMultidisciplinary Research Group in Nanoscience and Nanotechnology of the National University of Trujillo (GMIN-UNT).

^dMultidisciplinary Research Laboratory in Nanoscience and Nanotechnology "Ms. C. Oswaldo Roger Sánchez Rosales".
 Departament of Physics, National University of Trujillo, La Libertad, Perú
gzavaleta@unitru.edu.pe

Infections caused by *Escherichia coli* and *Staphylococcus aureus*, currently have a significant impact on human health. The objective was to synthesize, characterize and evaluate the antibacterial effect of Ag@ZnO nanoparticles at different concentrations on *E. coli* ATCC 25922 and *S. aureus* ATCC 25923. The nanoparticles were synthesized by a chemical route and characterized using dynamic light scattering (DLS), UV-visible spectrophotometry and transmission electron microscopy (TEM). Antibacterial susceptibility testing was performed using the agar diffusion method (modified Kirby -Bauer), minimum inhibitory concentration (MIC) and minimum bactericidal concentration (MBC). The results demonstrated the bactericidal and bacteriostatic activity of the nanoparticles on both bacteria.

1. Introduction

In recent years, microorganisms have been the source of many diseases, causing millions of deaths, and increasingly becoming a constant struggle for survival (Camacho, 2023). *Escherichia coli* is a bacterium that causes different intestinal and extraintestinal pathologies, it causes urinary tract infections, and is also found in the invasion of soft and cutaneous tissues (Mustapha & Goel, 2020). On the other hand, *Staphylococcus aureus* is an opportunistic pathogen, with significant impact on public health, its infections vary from mild cutaneous infections to more serious ones such as necrotizing pneumonia (Oliveira et al., 2018). The inappropriate use of medications, limited access to health care, and even medical malpractice have a negative impact on public health (Serwecińska, 2020). Thus, nanotechnology in the healthcare field (Cicci et al., 2017) has enabled the development of silver (Ag) and zinc oxide (ZnO) nanoparticles as antimicrobial agents (Khatami et al., 2018). ZnO, in its nanoparticle form, has high antibacterial activity (Daddy et al., 2021). However, for these nanoparticles to maintain their effectiveness, the presence of stabilizing agents is essential to prevent the agglomeration of Ag nanoparticles and preserve their antimicrobial properties (Bouafia et al., 2021). Thus, the use of hybrid Core-Shell nanoparticles, composed of two nanomaterials, where one nanoparticle serves as the core and the other as the shell (Zaleska et al., 2016). In this sense, the combination of Ag and ZnO nanoparticles provides enhanced bifunctional characteristics, along with improved dispersion and stability of Ag Nanoparticles (Li et al., 2021).

The objective of this study was to synthesize, characterize and evaluate the antibacterial effect of different concentrations of Ag@ZnO nanoparticles on *Escherichia coli* ATCC 25922 and *Staphylococcus aureus* ATCC 25923.

2. Methodology

2.1 Synthesis and characterization of nanoparticles

The synthesis was carried out via a two-stage chemical route. In the first phase, silver nanoparticles were synthesized by chemical reduction. A solution of silver nitrate (AgNO_3) in distilled water was first prepared, then heated and stirred constantly until a stable temperature of 90 °C was reached. Trisodium citrate, which acts simultaneously as a stabilizing and reducing agent at high temperatures, was added. After maintaining this mixture under constant stirring for 15 minutes, a yellow solution was obtained, indicative of the formation of silver nanoparticles.

In the second stage, the synthesized silver nanoparticles served as cores on which a shell of zinc oxide was deposited. To achieve this, the silver nanoparticles were added to a second aqueous solution of zinc acetate ($\text{Zn}(\text{CH}_3\text{COO})_2$) maintained at 70 °C under constant stirring. After 5 minutes of mixing, hexamethylenetetramine (HMT) was added as a stabilizing agent in the formation of ZnO.

Characterization was carried out by dynamic light scattering (DLS) using the Nicom system, UV-visible spectrophotometry using the Specord S-600 UV-vis spectrophotometer, and transmission electron microscopy (TEM) using the Thermo Scientific Talos F200i microscope, in both conventional TEM and high-resolution TEM (HR-TEM) modes.

2.2 Preparation of the inoculum

Bacterial cultures of *E. coli* ATCC 25922 and *S. aureus* ATCC 25923, both provided by the La Libertad Reference Laboratory in Peru, were used. These were subsequently activated in brain–heart infusion (BHI) broth and then plated on nutrient agar. A bacterial suspension was prepared in 0.9% physiological saline solution, adjusted to a turbidity equivalent to 0.5 on the McFarland scale (1.5×10^8 CFU/mL). The concentration was verified using a Specord S-600 UV-vis spectrophotometer at a wavelength of 625 nm (Clinical & Laboratory Standards Institute, 2022).

2.3 Modified Kirby-Bauer method

Wells of 6 mm in diameter were used instead of discs. A volume of 50 μL of Ag@ZnO nanoparticles at different concentrations was added to each well. Positive (Ag nanoparticles) and negative (ultrapure water) controls were also included. The plates were incubated at 37 °C for 24 hours, and the diameters of the inhibition zones for each bacterium were measured (Zavaleta et al., 2019).

2.4 Determination of the minimum inhibitory concentration

The microdilution method was used, in which 50 μL of the bacterial inoculum and 50 μL of Ag@ZnO nanoparticles at varying concentrations were added to each well. Positive controls (Ag@ZnO nanoparticles) and negative controls (bacterial inoculum only) were included. Resazurin (blue) at 0.01% was used as an indicator, adding 10 μL per well. The plates were incubated at 37 °C for 24 hours. A color change to pink indicated bacterial growth, while a persistent blue color indicated inhibition (García et al., 2021).

2.5 Determination of the minimum bactericidal concentration

From the microplate used to determine the MIC, samples were plated onto nutrient agar starting from the minimum inhibitory concentration. The plates were incubated at 37 °C for 24 hours (García et al., 2021).

2.6 Statistical Analysis

All experiments were performed in quintuplicate, ensuring the reliability and reproducibility of the results. Statistical analysis was conducted using analysis of variance (ANOVA) with Infostat 2020 (free version) to determine significant differences between treatments and blocks ($p < 0.05$). Tukey's multiple comparison test was also applied.

3. Results and discussion

3.1 Characterization of Ag@ZnO nanoparticles

Hydrodynamic size distribution

In Figure 1 (a) and (b), the hydrodynamic size distribution of Ag nanoparticles and Ag@ZnO nanoparticles is presented, showing an average diameter of 27.5 (a) and 46.0 nm (b), respectively.

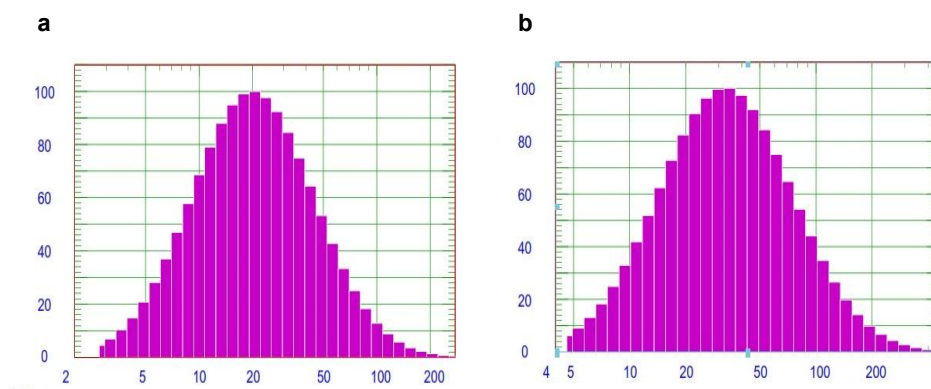


Figure 1: (a) Hydrodynamic size of Ag nanoparticles, measured by DLS. (b) Hydrodynamic size distribution of Ag@ZnO nanoparticles, measured by DLS.

UV-Visible Spectroscopy

In Figure 2, the silver plasmon resonance bands for each type of nanoparticle are clearly observed. The plasmon shift and slight decrease in intensity in Ag@ZnO nanoparticles are attributed to the presence of the ZnO shell.

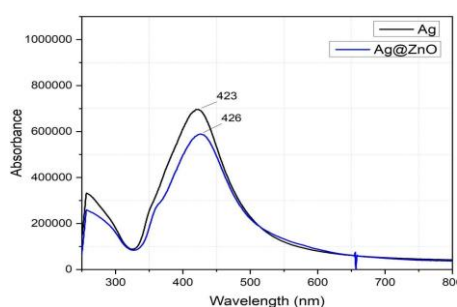


Figure 2: UV-vis absorption spectra of Ag and Ag@ZnO nanoparticles.

Transmission Electron Microscopy

Figure 3 (a) shows Ag@ZnO nanoparticles with diameters ranging from 15 to 25 nm. Figure 3 (b) provides a more detailed view of the shape of Ag@ZnO and the thin ZnO layer that surrounds the Ag core. Finally, Figure 3 (c), obtained by TEM, shows the presence of Ag nanoparticles with average diameters ranging from 15 to 20 nm.

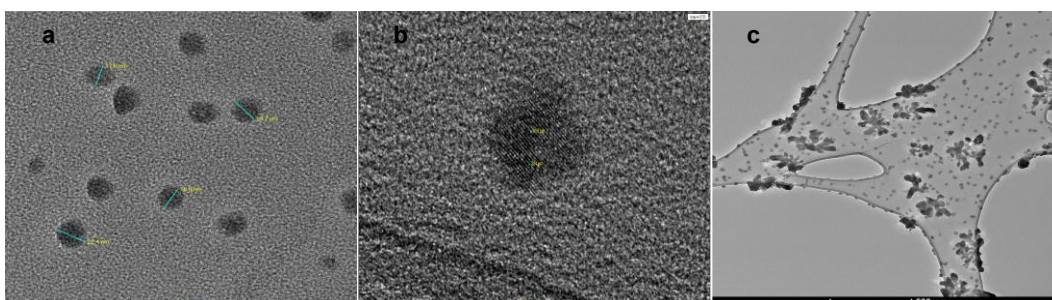


Figure 3: (a) TEM image of Ag@ZnO nanoparticles, at a scale of 20 nm. (b) HR-TEM image of Ag@ZnO nanoparticles, at a scale of 2 nm. (c) TEM image of Ag nanoparticles, at a scale of 500 nm.

Antibacterial Effect

Figures 4 (a) and (b) show the inhibition zones at different concentrations of core-shell Ag@ZnO nanoparticles against *E. coli* and *S. aureus*. These results indicate that higher concentrations produce greater antibacterial effects, suggesting there is a directly proportional relationship between the diameter of the halo and the concentration of the nanoparticles. As shown in Table 1, *E. coli* exhibited an inhibition diameter of 12.24 mm at 26.6 µg/mL, while *S. aureus* displayed a 7.88 mm halo at the same concentration. This indicates a stronger antibacterial effect against *E. coli*.

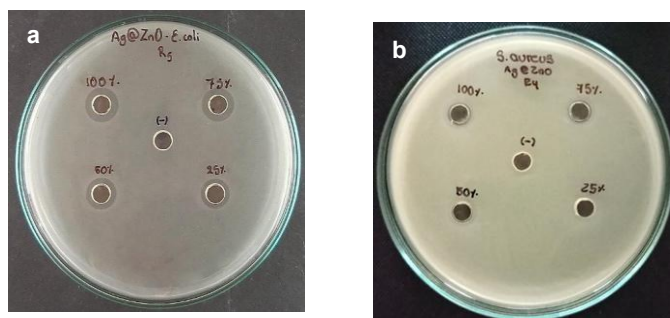


Figure 4: Bacterial growth inhibition halos at four concentrations of de Ag@ZnO nanoparticles on *Escherichia coli* ATCC 25922 (a) and *Staphylococcus aureus* ATCC 25923 (b).

Table 1: Inhibition halo diameters at different concentrations of Ag@ZnO nanoparticles on *Escherichia coli* ATCC 25922 and *Staphylococcus aureus* ATCC 25923.

Percentage	Concentration	Inhibition halo diameters (mm)	
(%)	(µg/mL)	<i>Escherichia coli</i>	<i>Staphylococcus aureus</i>
100	26.6	12.24	7.88
75	19.95	11.40	6.54
50	13.3	11.00	6.01
25	6.65	10.00	0.00

The results of this study differ from those reported by Khan et al. (2020), who found antibacterial activity of Ag@ZnO nanoparticles embedded in polyvinylpyrrolidone and polyvinyl alcohol hydrogels at concentrations of 25, 50, and 100 µg/mL against *S. aureus*, with inhibition halos of 8, 11, and 12 mm, respectively. Such variation has been attributed to differences in hydrogel types, synthesis methods, nanoparticle sizes, and concentrations. Another study using Ag@ZnO nanoparticles at 12.5 mg/mL against *E. coli* reported inhibition zones of 3.38 ± 1.93 mm, and 5.08 ± 3.39 mm for *S. aureus* (Aguilar et al., 2024). The greater inhibition found in our study, even at lower concentrations, suggests that these nanoparticles could serve as an effective alternative for bacterial control.

Table 2 presents the MIC and MBC values. Ag@ZnO nanoparticles were effective at low concentrations, with MIC values of 7.98 µg/mL for *S. aureus* and 5.98 µg/mL for *E. coli*, indicating that *E. coli* is more susceptible. Hashem & El-Sayyad (2023) reported MIC of 62.5 µg/mL for both bacteria, which is significantly higher than the values observed in this study, confirming the high efficacy of the nanoparticles synthesized herein.

Regarding the MBC, the nanoparticles eliminated 99.9% of the bacteria in *S. aureus* at a concentration of 7.98 µg/mL, while in *E. coli*, the concentration was 5.98 µg/mL, demonstrating its effectiveness compared to *S. aureus*.

Table 2: Determination of the minimum inhibitory (MIC) and minimum bactericidal concentration (MBC) of Core Shell Ag@ZnO nanoparticles on *Escherichia coli* ATCC 25922 and *Staphylococcus aureus* ATCC 25923.

Bacteria	MIC (µg/mL)	MBC (µg/mL)
<i>Escherichia coli</i>	5.98	5.98
<i>Staphylococcus aureus</i>	7.98	7.98

In other studies, ZnO/Ag nanoparticles exhibited MIC and MBC values of 1.5 µg/mL and 3.75 µg/mL, respectively, against *S. aureus* (Busila et al., 2023). Matai et al. (2014) reported strong bacterial inhibition at 550 µg/mL for *E. coli*, and MIC of 60 µg/mL for *S. aureus*. Likewise, Dutta et al. (2023) reported MIC and MBC values of 64 and 128 µg/mL, respectively, for ZnO-Ag nanoparticles.

Huang et al. (2020) used Ag@ZnO nanoparticles prepared with 0.3% oleic acid, achieving 99.9% bacterial elimination for both *E. coli* and *S. aureus*, and reported prolonged silver ion release.

Similarly, biosynthesized Ag–ZnO nanohybrids using aqueous extract of *Piper nigrum* showed an MIC of 100 µg/mL against *E. coli* (Mohapatra et al., 2023), further demonstrating the antibacterial potential of these nanocomposites.

These findings agree with the trend observed in this study, which showed higher efficacy against *E. coli* than *S. aureus*. This difference may be explained by the structural differences in bacterial cell walls: Gram-negative bacteria like *E. coli* have thinner peptidoglycan layers than Gram-positive bacteria such as *S. aureus* (Kim et al., 2020).

Ag⁺ and Zn²⁺ ions released from the nanoparticles disrupt the bacterial membrane through electrostatic interactions (Xiu et al., 2012), while the generation of reactive oxygen species (ROS) causes additional membrane damage, metabolic disruption, DNA fragmentation, lipid peroxidation, and ultimately cell death (Kumar et al., 2019).

Furthermore, the synergistic interaction between ZnO and Ag results in enhanced antibacterial activity with low cytotoxicity, as confirmed by Bradford protein assays and electron microscopy (Mohapatra et al., 2023). ZnO–Ag nanoparticles have also been shown to be more effective than individual ZnO nanoparticles (Zare et al., 2019), highlighting their therapeutic potential.

Based on these findings, Ag@ZnO nanoparticles show great promise as a future alternative to conventional antibiotics, particularly for addressing multidrug-resistant pathogens in hospital settings. Further research is warranted to explore their mechanisms of action and optimize their biomedical applications.

4. Conclusions

Ag@ZnO nanoparticles were synthesized using the chemical reduction method and characterized by DLS, UV-VIS spectroscopy, and TEM. The analyses confirmed the presence of characteristic Ag plasmon resonance bands and Ag@ZnO nanoparticles, with average sizes ranging from 15 to 20 nm.

At a concentration of 26.6 µg/mL, Ag@ZnO nanoparticles exhibited inhibition zones of 12.24 mm against *Escherichia coli* and 7.88 mm against *Staphylococcus aureus*, indicating a pronounced antibacterial effect.

The minimum inhibitory concentration (MIC) and minimum bactericidal concentration (MBC) were 5.98 µg/mL for *E. coli* and 7.98 µg/mL for *S. aureus*, confirming the bacteriostatic and bactericidal potential of Ag@ZnO nanoparticles.

Acknowledgments

The financial support provided by the CONCYTEC-World Bank Project “Improvement and Expansion of the Services of the National System of Science, Technology and Technological Innovation” 8682-PE, through its executing unit PROCIENCIA with contract No. 048-2019-FONDECYT-BM-INC.INV, is acknowledged, thanked and valued.

References

- Aguilar J., García-Zaleta D.S., Aguilar-Sánchez N.C., Velázquez-Martínez J., Hernández C., Martínez-Corona Z., 2024. Caracterización de nanomateriales de Ag, ZnO, y Ag/ZnO y su evaluación de propiedades antimicrobianas en *S. typhimurium*, *B. cereus*, *S. aureus* y *E. coli*, *Materiales Avanzados*, 4, 71–78.
- Bouafia A., Laouini S.E., Ahmed A.S., Soldatov A.V., Algarni H., Chong K.F., Ali A.M., 2021, The Recent Progress on Silver Nanoparticles: Synthesis and Electronic Applications, *Nanomaterials*, 11, 9, 2318.
- Busila M., Musat V., Alexandru P., Romanitan C., Brincoveanu O., Tucureanu V., Mihalache I., Iancu A.V., Dediu V., 2023, Actividad antibacteriana y fotocatalítica de nanocompuestos ZnO/Au y ZnO/Ag, *Revista Internacional de Ciencias Moleculares*, 24 (23), 16939.
- Camacho L., 2023, Resistencia bacteriana, una crisis actual. *Revista Española de Salud Pública*, 97.
- Cicci A., Sed G., Tirillo J., Stoller M., Bravi M., 2017, Production and Characterization of Silver Nanoparticles in Cultures of the Cyanobacterium *A. Platensis* (*Spirulina*), *Chemical Engineering Transactions*, 57, 1405–410.
- Clinical & Laboratory Standards Institute, 2022, *Performance Standards for Antimicrobial Susceptibility Testing*, (32nd ed.).

- Dadi R., Kerignard E., Traore M., Mielcarek C., Kanaev A., Azouani R., 2021, Evaluation of Antibacterial Efficiency of Zinc Oxide Thin Films Nanoparticles Against Nosocomial Bacterial Strains, *Chemical Engineering Transactions*, 84, 13–18.
- Dutta G., Chinnaiyan S.K., Sugumaran A., Narayanasamy D., 2023, Sustainable bioactivity enhancement of ZnO-Ag nanoparticles in antimicrobial, antibiofilm, lung cancer, and photocatalytic applications, *RSC Advances*, 13(38), 26663–26682.
- Garcia J., Afonso A., Fernandes C., Nunes F.M., Marques G., Saavedra M.J., 2021, Comparative antioxidant and antimicrobial properties of *Lentinula edodes* Donko and Koshin varieties against priority multidrug-resistant pathogens, *South African Journal of Chemical Engineering*, 35, 98–106.
- Hashem A.H., El-Sayyad G.S., 2023, Antimicrobial and anticancer activities of biosynthesized bimetallic silver-zinc oxide nanoparticles (Ag-ZnO NPs) using pomegranate peel extract. *Biomass Conversion and Biorefinery*, 14, 20345–20357.
- Huang X., Chen Y., Feng X., Hu X., Zhang Y., Liu L., 2020, Incorporation of oleic acid-modified Ag@ZnO core-shell nanoparticles into thin film composite membranes for enhanced antifouling and antibacterial properties. *Journal of Membrane Science*, 602, 117956.
- Khan I., Paul P., Behera S.K., Jena B., Suraj K., Lundborg C. S., Mishra, A., 2020, To decipher the antibacterial mechanism and promotion of wound healing activity by hydrogels embedded with biogenic Ag@ZnO core-shell nanocomposites, *Chemical Engineering Journal*, 128025.
- Khatami M., Varma R.S., Zafarnia N., Yaghoobi H., Sarani M., Kumar, V.G., 2018, Applications of green synthesized Ag, ZnO and Ag/ZnO nanoparticles for making clinical antimicrobial wound-healing bandages, *Sustainable Chemistry and Pharmacy*, 10, 9–15.
- Kim I., Viswanathan K., Kasi G., Sadeghi K., Thanakkasaranee S., Seo J., 2020, Preparation and characterization of positively surface charged zinc oxide nanoparticles against bacterial pathogens. *Microbial Pathogenesis*, 149, 104290.
- Kumar S., Majhi R.K., Singh A., Mishra M., Tiwari A., Chawla S., Guha P., Satpati B., Mohapatra H., Goswami L., Goswami, C., 2019, Carbohydrate-coated Gold-Silver nanoparticles for efficient elimination of multi drug resistant bacteria and in vivo wound healing, *ACS Applied Materials & Interfaces*, 11, (46) 42998–43017.
- Li W., Huang Z., Cai R., Yang W., He H., 2021, Rational Design of Ag/ZnO Hybrid Nanoparticles on Sericin / Agarose Composite Film for Enhanced Antimicrobial Applications, *International Journal of Molecular Sciences*, 22, (1), 105–118.
- Matai I., Sachdev A., Dubey P., Kumar S.U., Bhushan B., Gopinath P., 2014, Antibacterial activity and mechanism of Ag – ZnO nanocomposite on *S. aureus* and GFP-expressing antibiotic resistant *E. coli*, *Colloids and Surfaces B: Biointerfaces*, 115, 359–367.
- Mohapatra B., Mohapatra S., Sharma N., 2023, Biosynthesized Ag–ZnO nanohybrids exhibit strong antibacterial activity by inducing oxidative stress, *Ceramics International*, 49(12), 20218-20233.
- Mustapha M., Goel P., 2020, Isolation and prevalence of uropathogenic *E. coli* in different breed, sex and age of dogs, *Revue Vétérinaire Clinique*, 55(2), 49–54.
- Serwecińska L., 2020, Antimicrobials and antibiotic-resistant bacteria: A risk to the environment and to public health, *Water*, 12(12), 3313.
- Xiu Z., Zhang Q., Puppala H.L., Colvin V.L., Alvarez, P.J., 2012, Negligible Particle-Specific Antibacterial Activity of Silver Nanoparticles, *Nano Letters*, 12(8), 4271–4275.
- Zaleska A., Marchelek M., Diak M., Grabowska E., 2016, Noble metal-based bimetallic nanoparticles: the effect of the structure on the optical, catalytic and photocatalytic properties, *Advances in Colloid and Interface Science*, 229, 80–107.
- Zare M., Namratha K., Alghamdi S., Hussein Y., Mohammad E., Hezam A., Zare M., Drmosh Q.A., Byrappa, K., Novel Green Biomimetic Approach for Synthesis of ZnO-Ag Nanocomposite; Antimicrobial Activity against Food-borne Pathogen, Biocompatibility and Solar Photocatalysis, *Sci Rep.*, 9 (1), 8303.
- Zavaleta G., Saldaña J., Jáuregui S., Pacherez D., Rivera M., Samanamud F., 2019, Antibacterial effect of ZnO nanoparticles on *Staphylococcus aureus* and *Salmonella typhi*, *Arnaldoa*, 26(1), 421–432.